Inorganic Chemistry
Article

Inorg. Chem. **2010**, *49*, 4781–4790 **4781**
DOI: 10.1021/ic901617c

Investigation of the Structural Properties of an Extended Series of Lanthanide Bis-hydroxychlorides $Ln(OH)_2Cl$ (Ln = Nd−Lu, except Pm and Sm)

Ralph A. Zehnder,*,† David L. Clark,‖ Brian L. Scott,‡ Robert J. Donohoe,§ Phillip D. Palmer,‡ Wolfgang H. Runde,‡ and David E. Hobart*,‡,‖

†*Department of Chemistry, University of Louisiana at Monroe, Monroe, Louisiana 71209,* ‡*Chemistry Division,* §*Bioscience Division, and* ‖*Glenn T. Seaborg Institute for Transactinium Science, Los Alamos National Laboratory, Los Alamos, New Mexico 87545*

Received August 13, 2009

The trivalent lanthanide bis-hydroxychloride compounds, $Ln(OH)_2Cl$, (Ln = Nd through Lu, with the exception of Pm and Sm) have been prepared by hydrothermal synthesis starting with $LnCl_3 \cdot nH_2O$. These compounds were synthesized at temperatures not exceeding the melting point of the Teflon liners in the Parr autoclaves (∼220 °C). The compounds obtained were characterized by single crystal X-ray diffraction analysis, diffuse reflectance, FT-IR, and FT-Raman spectroscopies. Most of the lanthanide(III) bis-hydroxychlorides are isostructural and generally crystallize in the monoclinic space group $P2_1/m$. The bis-hydroxychlorides of the heavier lanthanide(III) atoms with smaller ionic radii also crystallize in the orthorhombic crystal system. Apparently hydrogen bonds between the OH groups and the Cl atoms connect the layers in the "c" direction. These H-bonds seem to be the driving force for the angle β of the monoclinic complexes to decrease with decreasing ionic radius of the Ln(III) ion and also for tying the layers together more strongly. As a result of this behavior, the structure of the heavier 4f analogues significantly resembles that of their orthorhombic counterparts. The heavier lanthanide bis-hydroxychlorides preferentially crystallize in the orthorhombic modification. The IR absorbance and Raman frequencies of the hydroxide ligands correlate as a function of the central lanthanide(III) ionic radius. This observation is corroborated by X-ray diffraction (XRD) structural data. These compounds are quite insoluble in near-neutral and basic aqueous solutions, but soluble in acidic solutions. It is expected that the analogue actinide bis-hydroxychlorides exhibit similar behavior and that this may have important implications in the immobilization and safe disposal of nuclear waste.

Introduction

The 4f elements commonly exhibit the trivalent oxidation state in solid state compounds, forming highly coordinated complexes with coordination numbers such as 8 and 9.[1] The decreasing ionic radius throughout the 4f series often results in a phase transformation accompanied by a decrease in coordination number. As a result of the decreasing ionic radius the space for coordination is lessened and, therefore, coordination numbers will vary from 9 to 8 to 6.[2] The 5f elements also exhibit the trivalent oxidation state, like the lanthanide elements.[2] Thus, it is expected that related actinide(III) complexes can be prepared by applying similar techniques and methods. A number of workers have shown that this is possible and that the structural and physicochemical properties of these 4f and 5f complexes compare well.[3−9] We, therefore, expect that the work described here can well be extended to the radioactive actinide elements and not only enhance the fundamental knowledge of f-element chemistry but also suggest implications for the long-term isolation and safe storage of spent nuclear fuels.

Previous spectroscopic investigations of an extended series of lanthanide oxalates,[10] inspired us to synthesize and structurally elucidate an extended series of lanthanide bis-hydroxychloride complexes. Thus, the direct comparison of

*To whom correspondence should be addressed. E-mail: zehnder@ulm.edu (R.A.Z.), dhobart@lanl.gov (D.E.H.). Phone: (+1)318-342-1836 (R.A.Z.), (+1)505-667-0205 (D.E.H.). Fax (+1)318-342-3334 (R.A.Z.), (+1)505-665-4737 (D.E.H.).

(1) Haschke, J. M. Halides. In *Handbook on the physics and chemistry of rare earths*; North Holland Pub. Co.: Amsterdam, 1979; Vol. *4*, pp 89−151.
(2) Kaltsoyannis, N. *The f elements*; Oxford University Press: Oxford, 1999.
(3) Del Cul, G. D.; Nave, S. E.; Begun, G. M.; Peterson, J. R. *J. Raman Spectrosc.* **1992**, *23*(5), 267–272.
(4) Del Cul, G. D.; Nave, S. E.; Peterson, J. R. *J. Alloy. Compd.* **1993**, *193* (1−2), 194–196.
(5) Fujita, D. K.; Cunningham, B. B.; Parsons, T. C. *Inorg. Nucl. Chem. Lett.* **1969**, *5*(4), 307–313.
(6) Peterson, J. R. *Nucl. Sci. Abstr.* **1968**, *22*(4), 6292.
(7) Peterson, J. R.; Cunningham, B. B. *J. Inorg. Nucl. Chem.* **1968**, *30*(3), 823–828.
(8) Schleid, T.; Morss, L. R.; Meyer, G. *J. Less-Common Met.* **1987**, *127*, 183–187.
(9) Templeton, D. H.; Dauben, C. H. *J. Am. Chem. Soc.* **1953**, *75*, 4560–4562.
(10) Morris, D. E.; Hobart, D. E. *J. Raman Spectrosc.* **1988**, *19*(4), 231.

Published on Web 05/12/2010

structural and physicochemical properties as a function of the decreasing ionic radius from the lighter to the heavier lanthanide complexes is realized. We have applied a synthetic methodology at relatively low temperatures, which has been generally successful in providing X-ray quality single crystals of the lanthanide bis-hydroxy chlorides.

Aksel'rud et al.[11−16] reported the preparation of Ln(OH)Cl_2, Ln$(OH)_2$Cl, and Ln$(OH)_3$, (Ln = Ce, Sm, Eu, Tb, Dy, Ho, Er, Yb, and Lu), as amorphous precipitates by simply titrating an aqueous lanthanide chloride solution with NaOH. These workers investigated the composition of the products as a function of pH while titrating the lanthanide (III) chlorides with NaOH. The synthesis of most lanthanide bis-hydroxychlorides, including crystallographic data, have been described by various scientists. Klevtsov et al.[17−19] reported the hydrothermal synthesis of the crystalline lanthanide bis-hydroxychlorides and their characterization via X-ray powder diffraction. Other authors performed X-ray single crystal structural studies on the La,[20] Pr, Sm, Gd,[21] and Nd[22,23] species. These workers determined that all of the bis-hydroxychlorides investigated were isostructural with monoclinic Y$(OH)_2$Cl.[24−27] However, some of these compounds were also found to crystallize in the orthorhombic crystal system with the space group *Pnma*.[18,19,24,26] All of these compounds were synthesized under various hydrothermal conditions, by reacting the rare earth oxides with $FeCl_3$ and/or NH_4Cl at temperatures between 300 and 600 °C.[17,18] These workers also isolated additional products such as $Ln_3O(OH)_5Cl_2$ and LnOOH at these temperatures. Carter et al.[28] found that the Ln$(OH)_2$Cl compounds are insoluble in water and dissolve very slowly in 6 M hydrochloric acid solutions at room temperature. It was also reported that temperatures above 375 °C lead to the decomposition of the Ln$(OH)_2$Cl species resulting in the formation of the corresponding oxychloride species.[29] Some recent articles illustrate the syntheses of nano crystals for the Ln$(OH)_2$Cl compounds with Ln = Er, Yb[30] as well as the generation of the Ln$(OH)_2$Cl [Ln = La−Yb] via solvothermal synthesis and successive decomposition into the oxychlorides at temperatures above 350 °C.[31,32] So far, no investigation concerning the correlation of the structural and spectroscopical properties of the extended series of lanthanide bis-hydroxychlorides has been discussed in detail. Elucidation of the chemistry of an extended series of Ln$(OH)_2$Cl complexes as a function of the ionic radius is expected to provide a clearer insight into their crystallographic structure. Extension of this work to the actinide elements may provide us with valuable information on the fundamental chemistry of the actinides and may provide a viable waste form for sequestering nuclear waste for long-term storage. In the present work, we describe the hydrothermal preparation of a series of lanthanide bis-hydroxychlorides, Ln$(OH)_2$Cl (Ln = Nd−Lu except Pm and Sm), starting with $LnCl_3 \cdot nH_2O$ at lower temperatures than reported previously. These compounds were characterized by single crystal X-ray diffraction analysis, diffuse reflectance, FT-IR, and FT-Raman spectroscopies.

Experimental Section

General Remarks. All chemicals used as starting materials were purchased from Acros Organics and Aldrich Co. and were used without further purification. Vibrational spectra were collected on a Thermo (Nicolet) combined FTIR/Raman bench using KBr pellets for the IR data, detected by a LN2-cooled MCT, and neat powders for the Raman experiments, detected by an InGaAs element. Spectral resolution was typically 2−4 cm^{-1}. Average data sets included 32 scans for the IR and 512 for the Raman. Some of the Raman spectra were obtained by using an argon-ion (UV) pumped stilbene dye laser at 416 nm and ∼10 mW. The signals were detected by a JY triple spectrograph with a Roper Scientific UV-enhanced LN2-cooled CCD using a resolution of ∼5 cm^{-1}. Diffuse reflectance spectra (see Supporting Information) were recorded using a Perkin-Elmer Lambda-19 UV−vis spectrophotometer and quartz reflectance cells.

Synthesis and Characterization. Samples of $LnCl_3 \cdot 6H_2O$ were weighed out and placed in Teflon liners inside Parr Acid Digestion vessels (Ln = Nd−Lu except Sm). Two models of Parr vessels were used, which are different in size. Model 4749, has a volume of 23 mL, while Model 4744 has a volume of 45 mL. Using the smaller vessel about 1 g of the respective lanthanide chloride hexahydrate was weighed out, while about 2 g of lanthanide chloride hexahydrate was weighed out for the larger sized vessel. Small amounts of deionized (DI) water was added (between 1 and 2 mL). Just enough to obtain a slurry of the respective salt inside the Teflon liner without dissolving noticeable amounts of the material. The vessels were then sealed and placed in a conventional laboratory oven at 220 °C for ∼21 days. At the end of the heating period the oven was switched off and the vessels were allowed to cool down slowly inside the closed oven, which took about 3−5 h to reach room temperature. Once at ambient temperature the Parr vessels were opened. Most commonly the materials obtained were entirely dry, while occasionally we obtained products, which were slightly wet. The resulting materials were transferred into 20 mL scintillation vials. Larger chunks of material were crushed into smaller pieces using a spatula. The vial was then filled with DI water, closed,

(11) Aksel'rud, N. V.; Ermolenko, V. I. *Zh. Neorgan. Khim.* **1961**, *6*, 777–782.
(12) Aksel'rud, N. V.; Spivakovskii, V. B. *Zh. Neorgan. Khim.* **1957**, *2*(12), 2709–2715.
(13) Aksel'rud, N. V.; Spivakovskii, V. B. *Zh. Neorgan. Khim.* **1958**, *4*, 56–61.
(14) Aksel'rud, N. V.; Spivakovskii, V. B. *Zh. Neorgan. Khim.* **1960**, *5*, 327–339.
(15) Aksel'rud, N. V.; Spivakovskii, V. B. *Zh. Neorgan. Khim.* **1960**, No. 5, 348–355.
(16) Aksel'rud, N. V.; Spivakovskii, V. B. *Zh. Neorgan. Khim.* **1960**, *5*, 547–557.
(17) Klevtsov, P. V.; Bembel, V. M.; Grankina, Z. A. *Zh. Strukt. Khim.* **1969**, *10*(4), 638–644.
(18) Klevtsov, P. V.; Kharchenko, L. Y.; Lysenina, T. G.; Grankina, Z. A. *Zh. Strukt. Khim.* **1972**, *17*(11), 2880–2883.
(19) Klevtsov, P. V.; Lysenina, T. G.; Kharchenko, L. Y. *Zh. Strukt. Khim.* **1973**, *14*(1), 87–91.
(20) Tarkhova, T. N.; Grishin, I. A. *Zh. Strukt. Khim.* **1970**, *15*, 2584–2586.
(21) Klevtsova, R. F.; Glinskaya, L. A. *Zh. Strukt. Khim.* **1969**, *10*, 494–497.
(22) Bukin, V. I. *Dokl. Akad. Nauk SSSR* **1972**, *207*, 1332–1335.
(23) Dem'yanets, L. N.; Emel'yanova, E. N. *Kristallografiya+* **1969**, *14* (4), 753–754.
(24) Jouve, C.; Marrot, J. D. R. *Acta Crystallogr.* **2002**, *C58*, i14–i15.
(25) Klevtsov, P. V. *C. R. Acad. Sci.* **1968**, *266*(6), 385–387.
(26) Klevtsov, P. V.; Klevtsova, R. F.; Sheina, L. P. *Zh. Strukt. Khim.* **1965**, *6*(3), 469–471.
(27) Klevtsova, R. F.; Klevtsov, P. V. *Zh. Strukt. Khim.* **1966**, *7*(4), 556–559.
(28) Carter, F. L.; Levinson, S. *Inorg. Chem.* **1969**, *8*(12), 2788–2791.
(29) Kipouros, G. J.; Sharma, R. A. *J. Less-Common Met.* **1990**, *160*(1), 85–99.
(30) Mahajan, S. V.; Hart, J.; Hood, J.; Everheart, A.; Redigolo, M. L.; Koktysh, D. S.; Payzant, E. A.; Dickerson, J. H. *J. Rare Earth* **2008**, *26*(2), 131.
(31) Hosokawa, S.; Iwamoto, S.; Inoue, M. *J. Alloy. Compd.* **2006**, *408−412*(9), 529–532.
(32) Hosokawa, S.; Iwamoto, S.; Inoue, M. *J. Am. Ceram. Soc.* **2007**, *90* (4), 1215–1221.

and shaken to wash the products and remove any soluble starting materials. The products were allowed to settle down at the bottom of the vial, and the water was decanted and discarded. This rinsing process was repeated three more times. The remaining products were composed of a mixture of crystalline materials that contained single crystals of X-ray quality as well as microcrystalline and/or amorphous powders. Small amounts of products were stored in scintillation vials with small quantities of DI water until a single crystal was chosen for X-ray structural analysis. The remaining materials were dried in a laboratory oven at 110 °C. The dry products were homogenized using a mortar and pestle and then characterized via FT-IR, Raman, and diffuse reflectance spectroscopies.

X-ray Structure Determination. Crystals were mounted in a nylon cryoloop using Paratone-N oil. The data were collected on a Bruker D8 APEX II charge-coupled-device (CCD) diffractometer, with a KRYO-FLEX liquid nitrogen vapor cooling device (140 K). The instrument was equipped with a graphite monochromatized MoKα X-ray source (λ = 0.71073 Å), with MonoCap X-ray source optics. Hemispheres of data were collected using ω scans. Data collection and initial indexing and cell refinement were handled using APEX II software. Frame integration, including Lorentz-polarization corrections, and final cell parameter calculations were carried out using SAINT+ software. The data were corrected for absorption using the SADABS program. Decay of reflection intensity was monitored by analysis of redundant frames. The structures (Table 1) were refined using non-hydrogen atom coordinates from isomorphous structures previously published[21,24] and on F^2 using the SHELXTL V6.1 package.[33,34] Hydrogen atom positions were either idealized or refined depending on the structure. Additional details of hydrogen atom treatment and software versions may be found in the Supporting Information CIF file.

Results and Discussion

Synthesis. The treatment of the various $LnCl_3 \cdot nH_2O$ compounds with small amounts of water under hydrothermal conditions at 220 °C for 21 days resulted in the formation of water insoluble products that formed either millimeter-sized crystals, amorphous solids, or a mixture of both. The crystal forms ranged from loose, thin, long individual needles to elaborate three-dimensional sprays or platelets.

With decreasing amounts of water present in the system, the formation of the product proceeds faster and produces higher yields. During some experiments, the autoclaves were apparently not completely sealed, so that water evaporated and left behind a higher yield of the product than in those cases when the product crystallized in fully sealed containers. The leakage of autoclaves seems to have been caused by the relatively high temperature of 220 °C at which Teflon starts to soften and deform. According to this observation we believe that one of the two following processes takes place:

1- The lanthanide chlorides first lose all their water of crystallization and then form the bis-hydroxychloride species via Reaction no.1 as it was proposed by Kipouros et al.,[29] who studied the dehydration of $NdCl_3 \cdot 6H_2O$.

$$LnCl_3 + 2H_2O \rightarrow Ln(OH)_2Cl + 2HCl \quad (1)$$

2- Other thermal decomposition studies regarding aluminum and magnesium hydroxy chloride analogues

Table 1. Crystal Data and Summary of Data Collection and Refinement for $Ln(OH)_2Cl$, Ln = Nd, Eu–Lu

Formula	$Nd(OH)_2Cl$	$Eu(OH)_2Cl$	$Gd(OH)_2Cl$	$Tb(OH)_2Cl$	$Dy(OH)_2Cl$	$Ho(OH)_2Cl$	$Er(OH)_2Cl$	$Tm(OH)_2Cl$	$Yb(OH)_2Cl$	$Lu(OH)_2Cl$	$Tm(OH)_2Cl$	$Yb(OH)_2Cl$	$Lu(OH)_2Cl$
fw	213.71	221.43	226.72	228.39	231.97	234.40	236.73			244.44	238.40	242.51	244.44
a (Å)	6.1980(7)	6.162(8)	6.1490(9)	6.152(1)	6.201(2)	6.213(1)	6.239(3)	6.214(1)	6.173(3)	6.1839(9)	12.563(1)	12.638(8)	12.609(3)
b (Å)	3.8710(5)	3.783(5)	3.7516(5)	3.7089(6)	3.650(1)	3.6224(7)	3.608(2)	3.5805(6)	3.5258(15)	3.5133(5)	3.5645(3)	3.556(2)	3.5093(8)
c (Å)	6.8103(8)	6.734(8)	6.7114(9)	6.659(1)	6.624(2)	6.616(1)	6.620(3)	6.572(1)	6.541(3)	6.5514(9)	6.2015(5)	6.221(4)	6.184(1)
α (deg)	90.00	90.00	90.00	90.00	90.00	90.00	90.00	90.00	90.00	90.00	90.00	90.00	90.00
β (deg)	113.308(2)	112.06(1)	111.597(2)	110.278(2)	108.028(2)	107.051(2)	106.277(4)	105.804(2)	105.393(4)	104.916(2)	90.00	90.00	90.00
γ (deg)	90.00	90.00	90.00	90.00	90.00	90.00	90.00	90.00	90.00	90.00	90.00	90.00	90.00
V (Å^3)	150.06(3)	145.5(3)	143.95(3)	142.53(4)	142.57(7)	142.36(5)	143.1(1)	140.70(4)	137.25(10)	137.54(3)	277.70(4)	279.6(3)	273.6(1)
space group	$P2_1/m$	$P2_1/m$	$P2_1/m$	$P2_1/m$	$P2_1/m$	$P2_1/m$	$P2_1/m$	$P2_1/m$	$P2_1/m$	$P2_1/m$	*Pnma*	*Pnma*	*Pnma*
Z	2	2	2	2	2	2	2	2	2	2	4	4	4
D_c	4.730	5.056	5.230	5.322	5.404	5.468	5.495	5.627	5.868	5.902	5.702	5.761	5.933
μ (mm^{-1})	17.918	22.198	23.680	25.461	26.856	28.440	29.997	32.188	34.745	36.563	32.616	34.111	36.755
F(000)	190	196	198	200	202	204	206	208	210	212	416	420	412
T (K)	140(1)	140(1)	140(1)	140(1)	140(1)	140(1)	140(1)	140(1)	140(1)	140(1)	140(1)	140(1)	140(1)
reflns. meas.	1656	1306	1597	1490	1566	1508	1335	1497	1564	1478	2723	1262	2435
reflns. indep.	421	400	398	392	397	392	347	375	379	388	401	307	393
R_{int}	0.0277	0.0482	0.0442	0.0254	0.0693	0.0280	0.0366	0.0228	0.0261	0.0287	0.0221	0.0102	0.0321
R1($I > 2\sigma$)	0.0196	0.0345	0.0261	0.0220	0.0294	0.0157	0.0242	0.0170	0.0246	0.0203	0.0170	0.0679	0.0259
wR2 ($I > 2\sigma$)	0.0538	0.0817	0.0651	0.0702	0.0732	0.0476	0.0557	0.0429	0.0630	0.0474	0.0447	0.2286	0.0754

(33) Sheldrick, G. M. *Acta Crystallogr.* **1990**, *A46*, 467.
(34) Sheldrick, G. M. *SHELXL-97, a computer program for crystal structure refinement*; University of Göttingen: Göttingen, Germany, 1997.

suggest that the respective metal chloride melts in its crystal water under hydrothermal conditions and loses all but one or two waters of hydration stepwise with increasing temperature. A complete dehydration of the metal chloride is generally not observed, instead the metal cation hydrolyzes in the remaining waters of hydration producing the hydroxy chloride complexes.[35−38] The formation of lanthanide bis-hydroxy chlorides would then take place via stepwise reactions 2 and 3.

$$LnCl_3 \cdot nH_2O \rightarrow LnCl_3 \cdot 2H_2O + xH_2O \quad (2)$$

$$LnCl_3 \cdot 2H_2O \rightarrow Ln(OH)_2Cl + 2HCl \quad (3)$$

Solid State Structures. Generally the lanthanide bis-hydroxychlorides are isostructural and crystallize in the monoclinic crystal system (space group $P2_1/m$). However, with increasing atomic numbers, the heavier lanthanides preferably crystallize in the orthorhombic morphology (space group *Pnma*). At the end of the 4f series the Tm, Yb, and Lu compounds crystallize more commonly in the orthorhombic crystal system. To our knowledge the single crystal structural analysis data for the monoclinic and orthorhombic modifications of $Yb(OH)_2Cl$, $Tm(OH)_2Cl$, and $Lu(OH)_2Cl$ have not been reported so far. Numerous trials synthesizing $Yb(OH)_2Cl$ by us resulted in the formation of the orthorhombic species. However, adding significant amounts of sodium chloride to the reaction mixture resulted in $Yb(OH)_2Cl$, crystallizing in both modifications. Only one single suitable monoclinic crystal was identified in the mixture that produced crystal structure data of sufficient quality. We experienced a similar situation with obtaining single crystals for the Lu analogue. Therefore, we were able to characterize these two monoclinic bis-hydroxy chlorides with single crystal X-ray analysis only. Without any powder X-ray diffraction (XRD) performed on the bulk samples, we cannot exclude that we obtained mixed phases for the lighter elements as well. However, the crystals of the lighter Ln-analogues picked for single crystal X-ray analysis consistently delivered the monoclinic phase, and the crystallographer did not visually spot any crystals that would suggest a different phase. For the heavier Ln-elements, we obtained both phases simultaneously. To be consistent with previous literature reports on the orthorhombic form of $\beta-Sm(OH)_2Cl$,[24] we name these complexes $\beta-Ln(OH)_2Cl$ to distinguish them from their monoclinic counterparts. Although the majority of these compounds have been described previously, we reinvestigated most of these complexes and determined the X-ray single crystal structures all at the same temperature of ~141 K. We were unable to obtain suitable products and single crystals of the Ce, Pr, and Sm compounds. Therefore, we use previously published crystal structure data by Klevtsov et al. and Klevtsova et al.[17,21] to enable us to compare the unit cell parameters along the entire lanthanide series (except for promethium) and correlate observed trends to the decreasing ionic radius throughout the 4f element series. Since these authors do not make any statements about the temperature at which they performed their data collection, we assume that their data were collected at room temperature, as it was probably most commonly done at the time of their publication. As the following figures show, their structural parameters fit nicely within the trends that we observe for the data we collected. More detailed parameters of the compounds synthesized in the present work and those of the previously reported complexes are given in Supporting Information, Table S1.

In proceeding from the light lanthanides to the heavier lanthanides a continuous decrease of the unit cell parameters "b" and "c" in the crystal structures can be observed. The angle "β" decreases from 113.30° for the Ce species to 104.91° for the Lu species. The space group for the monoclinic complexes is $P2_1/m$. These complexes form an extended three-dimensional lattice in which each lanthanide metal center is coordinated to eight neighboring atoms; 6 O-atoms and 2 Cl-atoms. Each Cl-atom is bound μ^2 to two- and each hydroxy group is bound μ^3 to three -Ln central atoms. Figure 1 (a) illustrates the resulting highly linked network of hydroxy groups, Cl atoms, and metal centers in the "ab" plane. These lattices form infinite Ln-Cl-Ln zig/zag chains along the "b" axis. Two of these chains run through one unit cell, so that each unit cell accommodates two complete formulas of $Ln(OH)_2Cl$. Figure 1 (b) also shows the three-dimensional nature of these lattices in the "ac" plane. The "ab" lattices are tied together by hydrogen bonds between the OH groups and the Cl atoms along the "c" axis.

It is noteworthy that the $Ln(OH)_2Cl$ complexes in both topologies are closely related to the $PuBr_3$ structural type,[39] forming coordination polyhedra that surround the central Ln atom as trigonal prisms, which are capped with two half-octahedra on two of the rectangular faces (Figure 2). Two pairs of O atoms are equivalent with respectively equal interatomic distances (OH1, OH2) and together with two equivalent Cl atoms they build the six corners of the trigonal prism. The remaining two O atoms that build the tips of the semioctahedra have individually different Ln−O bond distances. Thus, four of the six OH groups are coordinated in a non-equivalent manner to the central atom. The structural motifs of the monoclinic complexes are identical to each other and to that of monoclinic $Y(OH)_2Cl$.[27]

The trigonal prisms are placed infinitely on top of each other in direction "b". The Supporting Information, Figure S1 shows that the chains of trigonal prisms are staggered in direction "b", so that the two caps of one trigonal prism form the corners of respectively two other trigonal prisms.

The OH groups form hydrogen bonds with the Cl atoms of an adjacent lattice in direction "c", such that H1 and H1′ form H bonds to one Cl atom that they directly face, while H2 and H2′ respectively form bonds to the staggered Cl atoms in "b/c" direction as also outlined

(35) Buzagh-Gere, E.; Gal, S.; Simon, J. *Inst. Gen. Anal. Chem.* **1974**, *28*, 25–30.
(36) Matthes, F.; Haessler, G. *Z. Chem.* **1963**, *3*(2), 72–73.
(37) Petzold, D.; Naumann, R. *Freib. Forsch. A* **1979**, *A616*, 75–86.
(38) Petzold, D.; Naumann, R. *J. Therm. Anal.* **1980**, *19*(1), 25–34.
(39) Brown, D.; Edwards, J. *J. Chem. Soc., Dalton: Inorg. Chem.* **1972−1999**, *16*, 1757–1762.

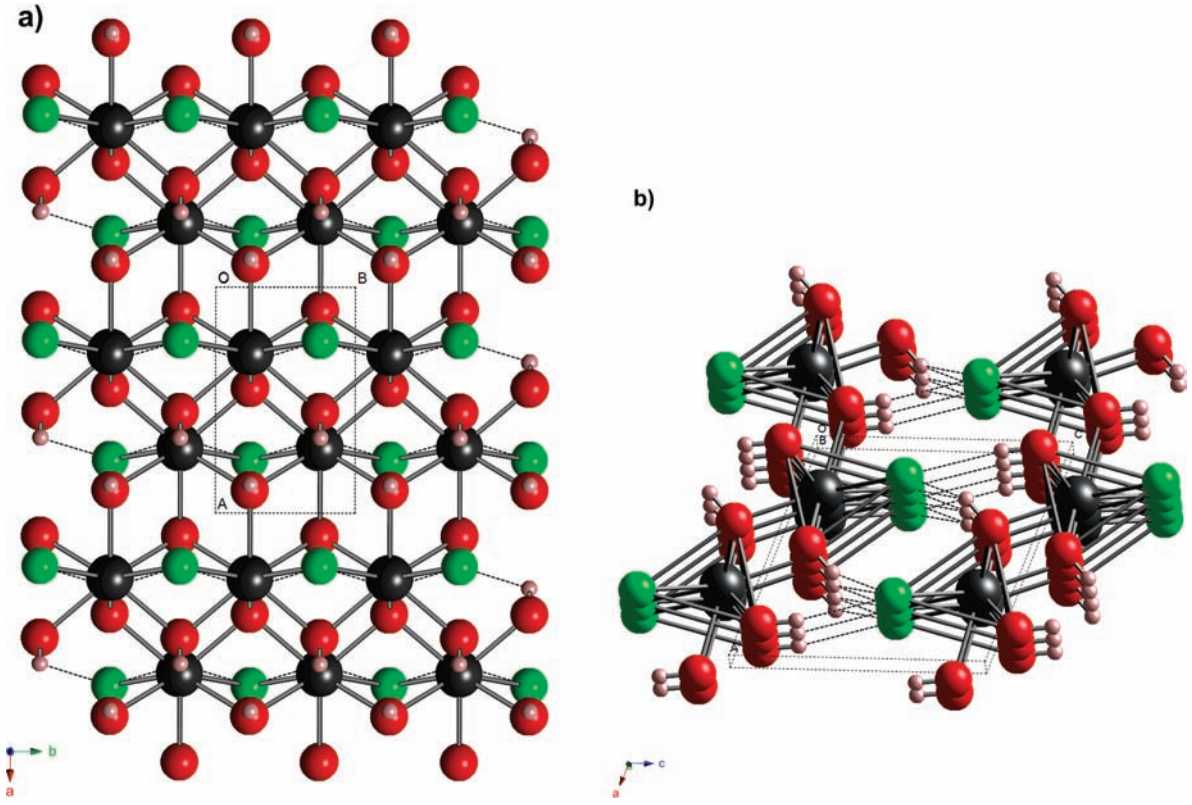

Figure 1. (**a**) Highly linked network of hydroxy groups, Cl atoms, and the metal centers in the ab plane of monoclinic $Dy(OH)_2Cl$. It clearly illustrates that each metal center is 8 coordinate, that each hydroxy group is coordinated to three metal centers, and that the metal centers form zig/zag chains with the chlorine ligands in the "b" direction. (**b**) Top view into the "b" direction of monoclinic $Tb(OH)_2Cl$, illustrating the role of OH1′ and OH2′ (Figure 2) serving as vertex for the semioctahedrons on two faces of the trigonal prisms. At the same time these OH groups are forming the corners of the adjacent staggered column of trigonal prisms. One can also recognize the two different kinds of H bonds in which these two OH groups are involved.

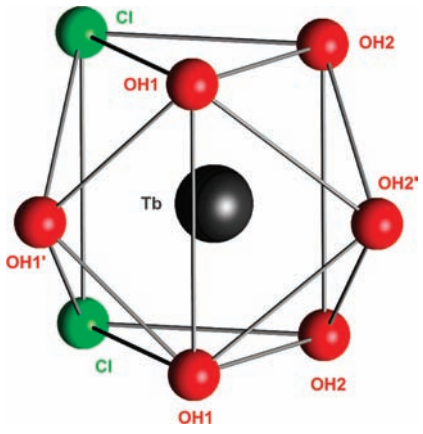

Figure 2. Coordination polyhedron of the Tb atom in monoclinic $Tb(OH)_2Cl$, showing the eight coordinate ligand environment, and using the atom numbering scheme as provided in the text and the crystallographic tables.

in Figure 1b and Supporting Information, Figure S1. It should be noted that, with decreasing ionic radius of the central atom along the series, two trends can be observed:

(1) The interatomic distances between the central atom and the six corners of the trigonal prism as well as the rear edge (Cl−OH2) and the vertical edges of the prism, connecting the equivalent groups (Cl−Cl, OH1−OH1, OH2−OH2), all follow a similar trend. They show a gradual decrease in length correlated to the decreasing ionic radius following the series from the lighter to the heavier lanthanide analogues. The same trend can be observed for the Ln−OH2 bond distance as well as for the hydrogen bonds between the H1, H1′ and the Cl atoms they face in the same plane. Figure 3 emphasizes the correlation between cell parameter *b* and the decreasing ionic radius of the lanthanide ion, which is also representative for the above-mentioned trends.

(2) A gradual decrease in length in correlation with the decreasing Ln ionic radius up to the Gd complex for the unit cell parameter *a* and all interatomic distances that point into direction "a", is observed. Between the Tb and Er analogues, a gradual increase in length is observed, followed by a gradual decrease between Er and Lu. Figure 3 also demonstrates these inconsistencies that occur because of the variation of the Ln−Ln distance in direction "a".

For comprehending this rather complicated trend, a closer look at the angle β of the monoclinic complexes and revision of the arrangements of the lattices and the coordination polyhedra is considerably useful. In the first half of the lanthanide series, the angle β decreases in very small increments between Ce (113.3°)[17] and Gd (111.6°). However, for the second half of the 4f series we observe a gradual decrease for β between Tb (110.28°) and Lu (104.92°), as can be seen in Figure 3.

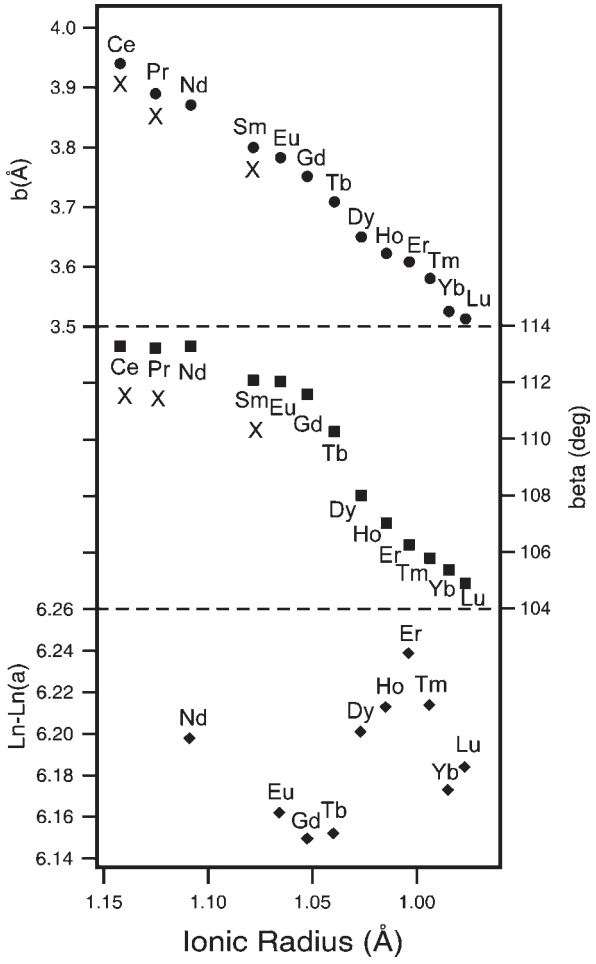

Figure 3. Cell parameter b (Å) in correlation with trivalent lanthanide-(III) ionic radius (Å),[40] (×: represents literature values, for references see Supporting Information, Table S1). Variation of β with decreasing ionic radius of Ln(III)[40] (×: represents literature values, for references see Supporting Information, Table S1). Interatomic distances between two Ln metal centers in direction "a" versus the trivalent lanthanide(III) ionic radius (Å).[40]

With the smaller angles for the heavier complexes the morphology more closely resembles the orthorhombic crystal structure, which correlates with the observation that these heavier analogues more readily crystallize in the orthorhombic morphology. With decreasing ionic radius, the orthorhombic modification seems to become energetically more favorable.

For a better understanding of the behavior of these complexes with respect to decreasing ionic radius of the central Ln atom, it is of interest to compare the lanthanide structures with the structure of the actinide compounds PuI_3 and $PuBr_3$, which both crystallize in the $PuBr_3$ structural type.[39] This shows that both modifications of the $Ln(OH)_2Cl$ complexes show close similarities with the $PuBr_3$[39] structural type. The molecular structure of $PuBr_3$[39] in the "ac" as well as in the "bc" plane is illustrated in the Supporting Information, Figure S2a and S2b.

In the view onto the "*ac*" plane one can see that the Pu central atoms are aligned straight in directions "a" and "c" and that the central atom is surrounded by 8-Br atoms that also form a similar coordination polyhedron as observed for the herein described compounds. This structure apparently arranges in a highly ordered formation because the central atom coordinates to only one kind of ligand. The repulsive effects between the bulky iodine atoms prevent this structure from crystallizing in the UCl_3 structure type,[41] in which the central atom is 9 coordinate. Because of the smaller ionic radius of the Cl atoms in this structure type the next halogen from the adjacent layer in direction "b" can actually form a ninth coordination to the central atom, which results in forming the tip of a third semi octahedron on the third rectangular face of the trigonal prisms of the coordination polyhedron. In the $PuBr_3$ structural type and the lanthanide bis-hydroxychloride compounds this third face remains uncapped because of the missing vertex caused by repulsive effects between the bromine ligands in $PuBr_3$ as well as the OH and Cl ligands in the $Ln(OH)_2Cl$ complexes and by space limitations. Looking at the orthorhombic crystal structure of $Lu(OH)_2Cl$ it becomes clear that the crystal lattice is arranged in a closely related manner as in $PuBr_3$ and that the Ln central atoms are aligned straight in directions "c" and "b" as illustrated in Figure 4. However, in the "a" direction, the central atoms form a zig/zag chain, whose center consists of a straight line pointing into direction "a". Thus, the neatly packed crystal lattice observed for $PuBr_3$ suffers a certain degree of distortion, which is caused by various effects. First, the central atom is coordinated to two different ligands in the $Ln(OH)_2Cl$ compounds, which show significant differences in their size. Another important aspect is that in these compounds we observe a competition between attractive forces that lead to hydrogen bonds in direction "c" and repulsive effects between the Cl and OH ligands.

By taking a closer look at Figure 4 one recognizes that two OH groups of each coordination polyhedron in the "ab" layer respectively are connected to one Cl atom of the adjacent "ab" layer by hydrogen bonds. This Cl atom is the missing vertex, which would form the third cap on the empty face of the trigonal prism in the next layer if it were arranged more closely to the Ln central atom of that layer. This would result in a 9 coordinate central atom and accordingly lead to a distorted form of the UCl_3 structural type.[41] However, the repulsive forces between this Cl atom and the four ligands building the corners of the empty face of the trigonal prism (2 Cl atoms and the two OH2 groups) prevent this bond formation as they keep the Cl atom at a distance of 3.722 Å from the Ln metal center as opposed to the actual Ln−Cl bond distances of 2.788 Å in β-$Lu(OH)_2Cl$.

The monoclinic molecular structure of $Lu(OH)_2Cl$ looks quite similar to that of the orthorhombic analogue (Figure 5).

Because of the angle β, which is 104.9° for monoclinic $Lu(OH)_2Cl$, one can observe a distortion of the crystal lattice as compared to β-$Lu(OH)_2Cl$. However, the monoclinic Lu species represents the closest approximation to the orthorhombic system for the entire 4f series.

At this point it is helpful to look at the series of $Ln(OH)_2Cl$ complexes and try to understand how the crystal lattice responds to the major changing effects throughout the 4f row as the ionic radius of

(40) Shannon, R. D. *Acta Crystallogr.* **1976**, *A32*, 751–768.
(41) Taylor, J. C. W., P. W. *Acta Crystallogr., Sect. B: Struct. Sci.* **1974**, *B30*(12), 2803–2805.

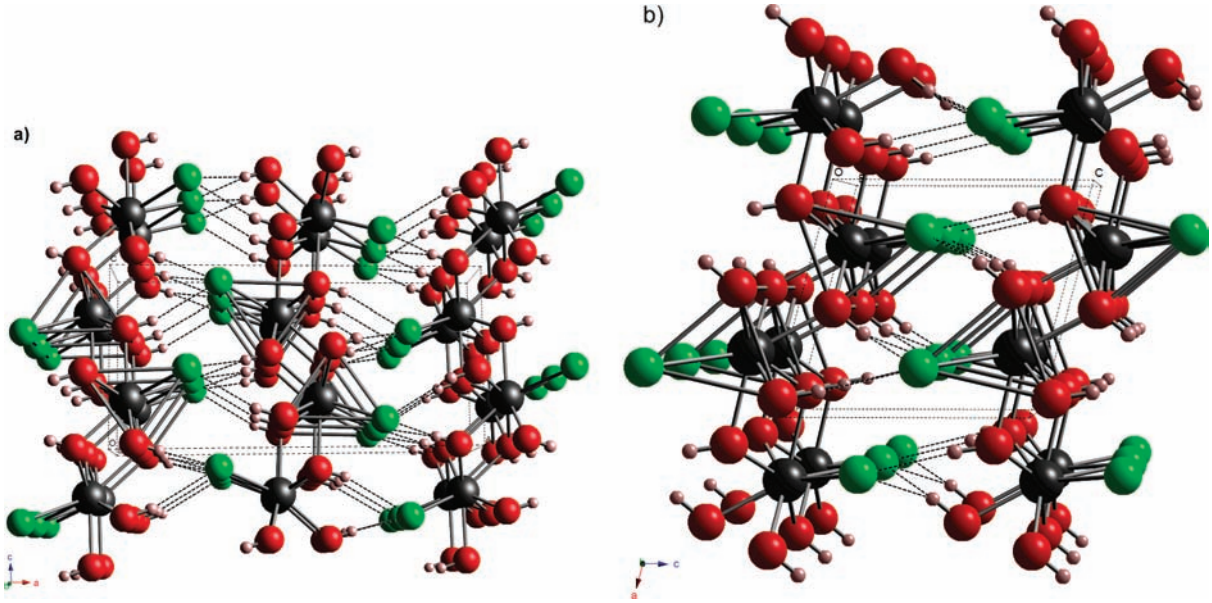

Figure 4. Crystal lattice of (**a**) orthorhombic $Lu(OH)_2Cl$ with a view onto the "ac" plane, showing the staggered arrangement of the central atoms; (**b**) monoclinic $Lu(OH)_2Cl$ in the ac plane showing that the central atoms are aligned straight in directions "c" and "b"; however, in direction "a" we see an even more distorted zigzag chain, which compensates for the effect that the angle β is not orthogonal.

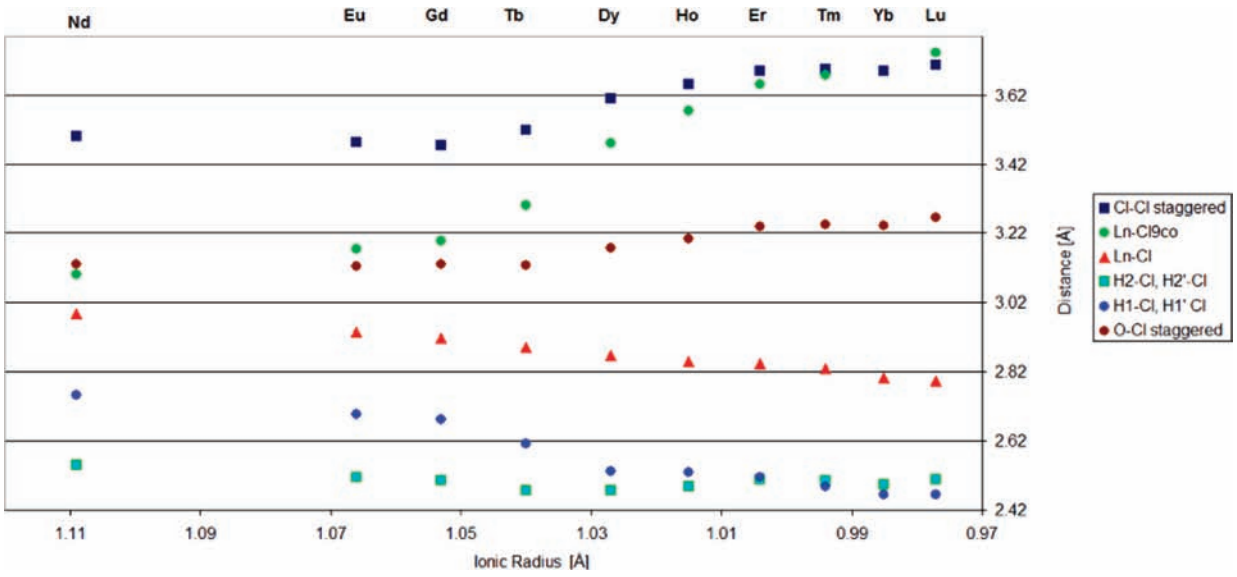

Figure 5. Trends of selected distances between the Cl atom of the adjacent layer in direction "c" and the atoms building the empty rectangular face of the coordination polyhedron it faces (including the Ln central atom) versus the trivalent lanthanide(III) ionic radius (Å).[40] Red triangle: the gradual trend of decreasing bond distance between the central atom and the two Cl ligands. Green diamond: Distance between the Ln central atom and the Cl atom of the adjacent layer. Blue square: Distance between the Cl ligands and the Cl atom of the adjacent layer, which is arranged in staggered formation. Brown diamonds: Distance between the OH2 ligands and the Cl atom of the adjacent layer, which is arranged in staggered formation. Blue dots: Hydrogen bond lengths between the H1,H1′ ligands and the Cl atom of the next layer. Green squares: Hydrogen bond lengths between the H2, H2′ ligands and the Cl atom of the adjacent layer.

the central atom gradually decreases with increasing atomic number.

Figure 5 illustrates the trends observed for the OH1, OH2′ hydrogen bond distances to the Cl atom of the adjacent layer and the distance changes between that Cl atom and the Ln central atom as well as the two OH groups and two Cl atoms building the uncapped third face of the trigonal prism.

It appears that the hydrogen bonds play a major role in tying together the adjacent layers in the "c" direction. With decreasing ionic Ln(III) radius the hydrogen bonds that are formed directly between the H1, H1′ and the Cl atoms facing each other at the same level of the adjacent layer decrease continually. However, the hydrogen bonds that are formed between one H2, H2′ and two Cl atoms arranged in staggered level formation slightly decrease between Nd and Tb and then slightly increase again between Tb and Lu. Thus, the Tb analogue possesses the shortest H2, H2′--Cl hydrogen bonds in the entire 4f row. This can be explained by the fact that the H2, H2′--Cl hydrogen bonds are twisted for the lighter $Ln(OH)_2Cl$ complexes as the Cl atom starts out at the corner of the

Table 2. Selected Parameters for Monoclinic $Ln(OH)_2Cl$ Compounds

OH_2-OH_2' [Å]	Cl−Cl [Å]	V [Å^3]	β [deg]	b [Å]	Ln−Ln^b [Å]	Ln−Ln^a [Å]
$Nd(OH)_2Cl$	2.843	3.871	150.06(3)	113.308(2)	3.8710(5)	6.198
$Eu(OH)_2Cl$	2.786	3.783	145.5(3)	112.060(14)	3.783(5)	6.162
$Gd(OH)_2Cl$	2.757	3.752	143.95(3)	111.5968(2)	3.7516(5)	6.149
$Tb(OH)_2Cl$	2.769	3.709	142.53(4)	110.278(2)	3.7089(6)	6.152
$Dy(OH)_2Cl$	2.739	3.650	142.57(7)	108.028(2)	3.6500(10)	6.201
$Ho(OH)_2Cl$	2.744	3.622	142.36(5)	107.051(2)	3.6224(7)	6.213
$Er(OH)_2Cl$	2.730	3.608	143.07(10)	106.277(4)	3.6085(15)	6.239
$Tm(OH)_2Cl$	2.699	3.58	140.70(4)	105.804(2)	3.5805(6)	6.214
$Yb(OH)_2Cl$	2.668	3.526	137.25(10)	105.393(4)	3.5258(15)	6.173
$Lu(OH)_2Cl$	2.664	3.513	137.54(3)	104.916(2)	3.5133(5)	6.184

[a] Ln−Ln distance along crystallographic *a* axis. [b] Ln−Ln distance along crystallographic *b* axis.

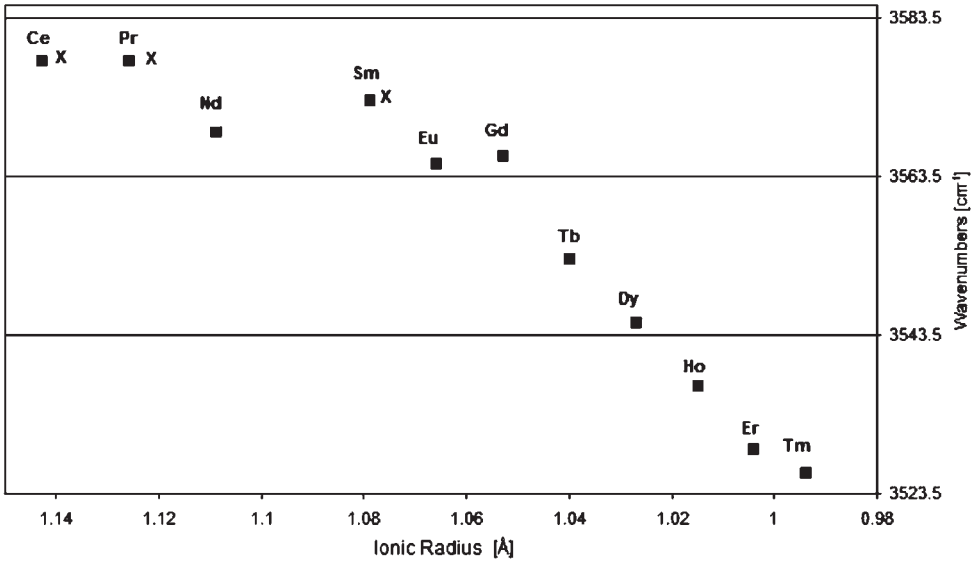

Figure 6. Correlation of the OH-I stretching modes with decreasing ionic radius.[40] The decreasing ionic radius causes the OH groups to merge closer to the Cl atoms, resulting in the strengthening of the H bonds. Therefore, the OH bonds weaken, and the stretching modes continuously decrease in energy, which can be confirmed by looking at the O−H and H−Cl bond distances of the XRD data, (×: represents literature values, for references see the Supporting Information, Table S1).

trigonal prism and then moving more into the center of the trigonal prism where they can be noticed as the missing vertex of the 9 coordinated polehedra, whose formation is prevented because the distance between those Cl atoms and the Ln metal centers increase with decreasing ionic Ln(III) radius. At the same time the Cl atoms start out on the left side of the H2, H2′ atoms that they face in a staggered manner. For the Tb analogue they have the most direct arrangement and for the heavier complexes the Cl atoms move farther to the right of the corresponding H2, H2′ atoms, which results in the twisting of the respective hydrogen bonds into the other direction.

For the first part of the series of lanthanide bis-hydroxychlorides only slight changes in the crystal strcture can be observed because the angle β does not decrease significantly in this region. However, beyond Gd a significant increase in distance can be recognized between the Cl atom of the adjacent layer and the other atoms of the uncapped side of the trigonal prism as the ionic radius of the central atom decreases and β significantly becomes smaller. As a result the crystal lattice responds to the changes for β as well as for the decreasing ionic radius by increasing the distance to the adjacent Cl atom, which results in the characteristic trends observed for

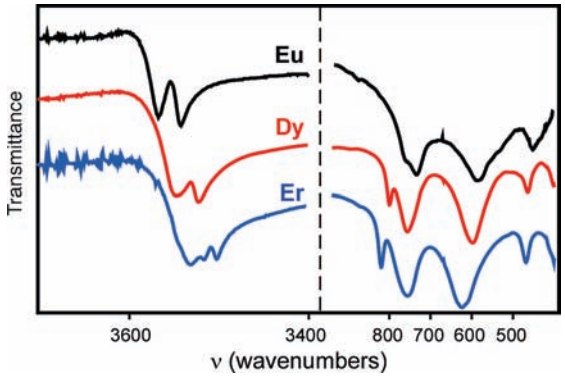

Figure 7. Selection of IR spectra showing the OH stretching and deformation modes of $Ln(OH)_2Cl$, in the order of decreasing ionic radius with Ln = Eu, Dy, Er.

the parameters in direction "a". These individual adjustments enable the lattice to decrease constantly its density, which can be found in reconciliation with the trend of the cell volume. The plot of the cell volume, shown in the Supporting Information, Figure S3, indicates that all changes in the lattice seem to be compensated well without a change in morphology by adjusting the above-discussed parameters. There is only a small inconsistency in the gradual decrease

Table 3. Infrared Vibrational Frequencies for Monoclinic $Ln(OH)_2Cl$ Compounds [cm^{-1}]

complex	ν OH $_{I}$	ν OH $_{II}$	ν OH $_{II'}$	δ OH $_{I}'$	δ OH $_{I,I'}$	δ OH $_{II, II'}$	Ln−Cl
$Ce(OH)_2Cl$[17]	3578	3558			720	567	
$Pr(OH)_2Cl$[21]	3578	3557			722	570	
$Nd(OH)_2Cl$	3569	3547			727	561	437
$Sm(OH)_2Cl$[21]	3573	3550		755	736	584	
$Eu(OH)_2Cl$	3565	3540		754	730	582	449
$Gd(OH)_2Cl$	3566	3542		766	736	588	452
$Tb(OH)_2Cl$	3553	3529		781	741	593	460
$Dy(OH)_2Cl$	3545	3521		799	757	598	464
$Ho(OH)_2Cl$	3537	3518	3501	810	749	615	465
$Er(OH)_2Cl$	3529	3515	3500	819	757	624	469
$Tm(OH)_2Cl$	3526	3509	3498	829	762	628	471

of the cell volume between the Tb and Er analogues that apparently remains within a range that can be accommodated by the monoclinic crystal lattice.

The unit cell density (not shown) increases very gradually with decreasing ionic Ln(III) radius. The most characteristic parameters that change as functions of decreasing ionic radius are listed in Table 2.

It is remarkable that the distance between the Ln metal center and the adjacent Cl atom (which represents the missing vertex of the third semi octahedron) becomes as close as 3.102 Å for the $Nd(OH)_2Cl$ complex, which is only slightly longer than the actual distance of 2.989 Å between the Ln central atom and the two equivalent Cl ligands for this compound. The observed properties are in contrast to the reported lanthanide borate complexes, in which a change in crystal structure takes place twice within the 4f row. These compounds exhibit the same structure type as the three forms of $CaCO_3$ aragonite, vaterite, and calcite. The first change in crystal structure is detected between Neodymium and Samarium. The Borates of La, Pr, and Nd crystallize in the aragonite type and the analogue compounds from Sm throughout Yb crystallize in the vaterite type. $LuBO_3$ crystallizes like $InBO_3$ in the calcite type.[42] In the larger lighter lanthanide borates the central atom is 9 coordinate and bound to three monodentate and three bidentate trigonal planar borate anions while the smaller heavier analogues are 8 coordinate with 2 bidentate and 4 monodentate tetrahedra.[42] However, in case of the $Ln(OH)_2Cl$ species each central atom is eight coordinate and because of the absence of large space filling ligands these complexes are able to gradually increase the density of the highly linked network by creating a customized fit for each complex, absorbing the strain on the crystal lattice that is created by the decreasing angle β. For the $Lu(OH)_2Cl$ species the most convergence between the orthorhombic and the monoclinic modifications can be observed, as shown in Figure 4.

We also observed that the $Ln(OH)_2Cl$ complexes show a remarkable stability in neutral and weak acidic environments. The complexes are stable in near neutral pH water, and they dissolve quite slowly in 0.1 M hydrochloric acid solutions, considering the fact that they are basic compounds. A crystalline sample of $Gd(OH)_2Cl$, for instance, did not entirely dissolve in a 0.02 M HCl solution within 4 weeks. We attribute this extraordinary inertness to the tight three-dimensional lattice system, which seems to control the reaction of these complexes kinetically and to slow down the dissolution rate in acidic media significantly.

Spectroscopic Studies. Vibrational Data. Most of the $Ln(OH)_2Cl$ compounds were characterized by FT-IR and Raman spectroscopies. All spectra look similar to the ones reported previously for $Ln(OH)_2Cl$ complexes[17] as well as for $Y(OH)_2Cl$.[26]

The four non-equivalent Ln−OH distances of each $Ln(OH)_2Cl$ species are represented by two degenerate deformation modes between 550 cm^{-1} and 600 cm^{-1} and between 700 cm^{-1} and 850 cm^{-1} for the lighter $Ln(OH)_2Cl$ complexes. However, with decreasing Ln−OH distances in the heavier species the mode between 700 cm^{-1} and 850 cm^{-1} representing the two equivalent OH-1 groups and the OH-1′ group splits into two separate bands, while the OH-2 and OH-2′ groups are represented by one single degenerate band throughout the 4f series. Klevtsov reported the separation of these modes occurring as a small shoulder from samarium onward.[17] We observed the same trend starting at europium (since we did not obtain any data for Sm). This shoulder finally evolves into a distinct separate band from the Ho analogue onward. All O−H deformation bands shift to higher energies with decreasing ionic radius. After the degenerate deformation values for OH-1 and OH-1′ split into separate modes from Sm[17] on, they continuously move farther apart from each other, as the ionic radius decreases with the heavier analogues, which can be seen in the Supporting Information, Figure S4. The stretching modes show quite similar behavior. The lighter ones show two modes between 3400 and 3600 cm^{-1} in the IR as well as the Raman spectrum. However, from Ho onward, an additional stretching mode can be observed, growing in as a shoulder first and eventually forming a distinct separate band. In contrast to the deformation modes, the stretching frequencies decrease in energy with decreasing ionic radius as demonstrated in Figure 6. This is in good agreement with the gradually decreasing H bond lengths going along with decreasing ionic Ln(III) radius.

With the shortening of the hydrogen bonds, the O−H bond distances increase and therefore, the respective energies of the stretching bands decrease. With increasing hydrogen bond strength the twisting of the OH groups becomes more restricted and therefore, the deformation modes increase in energy accordingly as the ionic Ln(III) radius decreases. These trends are illustrated in Figure 7, where we display the IR spectra of the Eu, Dy, and Er compounds. Because of the difficulties in producing the monoclinic form of $Yb(OH)_2Cl$ and $Lu(OH)_2Cl$ we were unable to obtain samples pure enough to determine the

(42) Giesber, H.; Ballato, J.; Chumanov, G.; Kolis, J.; Dejneka, M. *J. Appl. Phys.* **2003**, *93*(11), 8987–8994.

FT-IR and Raman spectra for the monoclinic species. Thus, we are not showing the IR data for these two compounds in Table 3.

Conclusion

We applied a hydrothermal synthesis method utilizing similar conditions to produce an extended series of Ln-$(OH)_2Cl$ complexes at lower temperatures than previously reported. We synthesized the lanthanide bis-hydroxychlorides from Nd through Lu, with the exception of Pm and Sm, applying the above-described method to obtain reproducible X-ray quality single crystals. Using the literature data previously published for the Ce, Pr, and Sm compounds we were able to compare the crystal structural data and the vibrational spectroscopy data of the $Ln(OH)_2Cl$ complexes of the entire 4f series (with the exception of Pm). Comparing the structural trends of these compounds throughout the series for the first time provided us with an interesting insight into the properties of the resulting extended lattices. These complexes are structurally related to $PuBr_3$,[39] and they crystallize in three-dimensional extended lattices that form infinite chains along the *b* axis. The lanthanide atom is surrounded by eight coordinate polyhedra. A shortening of the interatomic distances and varying polyhedra edge lengths as well as varying unit cell parameters along the 4f series compensate for the decreasing ionic radius and the increasing strain on the crystal lattice caused by the decreasing angle β along the series. This behavior seems to enable these compounds to crystallize in the monoclinic crystal system throughout the entire series. Because the crystal system becomes more similar to the orthorhombic crystal system, the crystal lattice suffers a certain degree of distortion for the complexes between Tb and Er because of the competition between decreasing bond distances and the repulsion between Cl atoms and OH groups as they move closer together. This effect, however, is compensated by corresponding variations of several parameters along the crystallographic *a* axis. The heavier analogues (Tm−Lu) crystallize more commonly in the orthorhombic morphology. This is in reconciliation with the general trend of the monoclinic species resembling the orthorhombic analogues more because of the decreasing angle β with increasing atomic number. Both morphologies crystallize in a distorted form of the 8 coordinate $PuBr_3$ structural type.[39] Because of the attracting and repelling forces between the ligands in adjacent layers and the fact that the central atoms are surrounded by two different ligands, the Cl atoms of one layer are prevented from forming a third cap of an additional semi octahedron on the empty face of the trigonal prism in the coordination polyhedron. If these Cl atoms were arranged more closely to the Ln central atom of the adjacent layer they would fill that missing third vertex. In that case the lanthanide bis-hydroxychlorides would form 9 coordinate coordination polyhedra and crystallize in a distorted form of the UCl_3 structural type.[41] The driving force for the monoclinic species to decrease the angle β and, therefore, increasingly resemble the orthorhombic counterparts with decreasing ionic radius seem to be the attractive forces between the H atoms and the Cl atoms. This results in the formation of hydrogen bonds tying together adjacent layers along the *c* axis. As the ionic radius decreases for the heavier $Ln(OH)_2Cl$ complexes, the hydrogen bonds increase in strength resulting in a phase transformation preferring the orthorhombic over the monoclinic modification. Either modification can be obtained depending on the mineralizing conditions of the individual experiments. This is in reconciliation with the decreasing hydrogen bond lengths and the decreasing energies of the O−H stretching modes observed in the IR and Raman spectra of the monoclinic complexes.

The highly linked three-dimensional network seems to contribute to the remarkable inertness of these compounds in near neutral aqueous environments. This could be one of the key properties for the potential application of actinide bis-hydroxychlorides as nuclear waste forms and might be further evaluated by testing other lanthanide mixed hydroxide complexes. Leachability experiments that we intend to perform in the near future will reveal if these compounds exhibit favorable properties for such purposes. We are planning to conduct similar hydrothermal synthesis experiments with some actinides such as Am and Cm. Since Am and Cm prefer the trivalent oxidation state and are quite similar to the lanthanides in their chemical properties, we anticipate success in synthesis of these actinide bis-hydroxychloride complexes. The radiolysis effects of these elements, however, may create difficulties in obtaining single crystals for X-ray analysis.

Acknowledgment. This work was supported at Los Alamos by the Division of Chemical Sciences, Geosciences, and Biosciences, Office of Basic Energy Sciences, U.S. DOE, and the, Glenn T. Seaborg Institute at Los Alamos. Los Alamos National Laboratory is operated by Los Alamos National Security, LLC, for the National Nuclear Security Administration of the U.S. Department of Energy under contract DE-AC52-06NA25396. We also thank Dr. Brendan Twamley (Dublin City University, Dublin, Ireland) and Dr. Thomas Fanghänel (Institute for Transuranium Elements, in Karlsruhe, Germany), for helpful comments and discussions. We dedicate this article to the memory of our esteemed co-author Dr. Robert J. Donohoe.

Supporting Information Available: Tables S1 and S2, Figures S1−S4, and crystallographic data in CIF format. This material is available free of charge via the Internet at http://pubs.acs.org.